

## Synthesis and characterization of new derivatives of CMC-g-PVA and evaluation pharmaceutical release, antibacterial activity, molecular docking

Rasha Shakere Nayyef<sup>1</sup>, Sana hitur Awad<sup>2\*</sup>

<sup>12</sup>Department of Chemistry, College of Science for Women, University of Baghdad, Baghdad, Iraq.

Email ID: [Rasha.Abd2305m@csw.uobaghdad.edu.iq](mailto:Rasha.Abd2305m@csw.uobaghdad.edu.iq)

Email ID: [sanaha\\_chem@csw.uobaghdad.edu.iq](mailto:sanaha_chem@csw.uobaghdad.edu.iq)

Cite this paper as: Rasha Shakere Nayyef, Sana hitur Awad, (2025) Synthesis and characterization of new derivatives of CMC-g-PVA and evaluation pharmaceutical release, antibacterial activity, molecular docking. *Journal of Neonatal Surgery*, 14 (4s), 675-687.

### ABSTRACT

In this research drug polymers, have been prepared by substituting drugs to polymers backbone, which raised interest as a result of the benefits systems possesses, as the first part of a continued research on conversion of carboxymethyl cellulose (CMC) to useful biopolymer-based materials, it possesses a plethora of other noteworthy attributes like biocompatibility, renewability, nontoxicity, and biodegradability, large numbers of hydroxyl functional groups were introduced onto CMC with different drugs (sulfamethoxazole, Salbutamol phenylephrin, Sodium Fusidate, Hemayoxiline, chloramphenicol) by grafting with polyvinyl alcohol. Evidence of prepared compound was obtained by FTIR spectra, HMR, UV visible, the CMC-g-PVA copolymer was characterized thermally by using differential scanning calorimetry and thermogravimetric analysis methods. The biological activity of the prepared pharmaceutical polymers against two types of bacteria was also studied. The molecular bonding of some of the prepared polymers was also studied. The pharmaceutical degradation of some of them was studied in different acidic and alkaline media.

The controlled release for all polymers was studied in different pH=4, pH=9 values at (30-40)<sup>0</sup>C. The hydrolysis data showed that release rates are strongly dependent on the pH of the medium and temperature. We concluded that the drug polymers could enhance the solubility of drug carrier polymers in water, with desirable properties, slow-release, and prolonged activity. These four methods of advanced properties and bearing of the different bioactive units, and studying Molecular Docking.

**Keywords:** Polyvinylalcohol, phthalicanhydride, Trimethoprim, Sodium Fusidate, Hemayoxiline, chloramphenicol, phenylephrine

### 1. INTRODUCTION

The carboxymethylation of hydroxyl groups in cellulose is the usual process that forms CMC (Kumar & Negi, 2018). Because hydroxyl and polar carboxylate groups are present, CMC exhibits great water solubility, hydrophilicity, and chemical reactivity. In addition, it possesses a plethora of other noteworthy attributes like biocompatibility, renewability, nontoxicity, and biodegradability (Saha *et al.*, 2019). Applications for carboxymethyl cellulose (CMC) include food production and medical therapies (Rahman *et al.*, 2021). It is frequently used in food and non-food goods to stabilize emulsions and act as a thickening or viscosity modifier. Since its main sources are either cotton linter or softwood pulp, it is mostly employed because of its high viscosity, nontoxicity, and overall hypoallergenic reputation (Elena-Emilia *et al.*, 2021). Along with being used in food products, it is also utilized in non-food items like laxatives, diet pills, detergents, water-based paints, textile sizing, reusable heat packs, different paper products, filtration materials, synthetic membranes, wound healing applications. Food fraud, shrimp and prawns: In order to deceive short-weight clients, CMC injections have been used to artificially raise the weight and aesthetic appeal of shrimp and prawns (Jiamin *et al.*, 2022). CMC is used in textile applications to help thicken printing pastes, improving the accuracy of the prints itself. Dyes can also be thickened using it. It also serves as a substitute for artificial thickeners (Sirajudheen *et al.*, 2020). In recent years, CMC and its numerous composites have garnered a great deal of attention. past 20 years, CMC-based hybrid composites especially their hydrogels have shown some encouraging results in the removal of various inorganic metal ions, including heavy metals in their complex ionic states (Zong *et al.*, 2019), dye pollutants (Kong *et al.*, 2020; Sirajudheen *et al.*, 2020), and even some radionuclides (Tanzifi *et al.*, 2020) from water treatment processes, from various contaminated waters. Application in the Water Treatment Process. In the present day, water pollution has become one of the most crucial issues worldwide. An immense number of pollutants come from various industries and household deeds every day and enter into aquatic environments, which further causes several types of disorders in different living organisms and human beings.

There is no absolute limit on how many types of pollutants can be present in wastewater that has come from multiple industries or other household activities. However, to the best of the author's knowledge, CMC-based materials have been mainly used thus far for the removal of various organic-inorganic dyes (Godiya *et al.*, 2020), diverse radioactive species (Awad *et al.*, 2021), as well as inorganic ionic contaminants (both anions and cations) (Janarthanan *et al.*, 2020) from contaminated waters under varied experimental circumstances in aquatic ecosystems, dyes are thought to be the most dangerous substances (Al-Sahib & Awad 2022). Waste dye effluents are now an essential component of wastewater treatment processes due to their extensive range of applications in several industries, including food, paint, textiles, pulp, paper, rubber, plastics, tanneries, cosmetics, and dozens of manufacturing and construction industries (Liu *et al.*, 2016).

## 2. MATERIALS AND METHODS

Polyvinylalcohol and phthalicanhydride, thionyl chloride, Dimethyl-sulphoxide(DMSO), Ethanol absolute from Fluka company and sulfamethoxazole, Salbutamol, phenylephrine, Trimethoprim, Hematoxylin, Sodium Fusidate, chloramphenicol. From the state company for drug industry and medical appliances Samarra(SDL).

### Experimental

In this investigation, all chemicals of the highest purity and supplied without further purification. Melting points were measured by Stuart melting points. The spectra Fourier transfer Infra-Red (FT-IR) spectra recorded using KBr disk, and  $^1\text{H}$ -NMR in Dimethylsulphoxide (DMSO) A Varian-400MHz spectrometer with TMS(Tetra methyl silane) as a reference was used to capture  $^1\text{H}$ -NMR.

### Preparation of PVA-grafted –CMC (S1)

1gm of PVA was dissolved in ethanol absolute: water (1:1) ml. (0.02 mole 2.96 gm) of phthalic anhydride was dissolved in 5ml of ethanol absolute, 2ml of dilute  $\text{H}_2\text{SO}_4$  was added, then mixture was refluxed for 6 hours  $70^\circ\text{C}$  and dry it at room temp, purify with ethanol. One gm of (PVA-g-pha), dissolved in 5ml of DMSO, 2ml of thionyl chloride was added and refluxed about 1/2 hr, then mixed with (1.31gm) of CMC dissolved in 5ml ethanol and refluxed about 8 hr, the product dry it and purified with ethanol absolute.

Preparation of sec-butyl ((2R,3R,4S,6S)-4-hydroxy-6-((2-((4-(N-((Z)-1-imino-3-methoxybut-2-en-1-yl) sulfamoyl) phenyl) amino)-2-oxoethoxy) methyl)-2-methoxy-5-methyltetrahydro-2H-pyran-3-yl) phthalate

Seven new drug polymers were prepared by substitution of S1 copolymer with some antibiotics. (1gm) of (S<sub>1</sub>) dissolved in 5ml of DMSO, mixed with (0.002mole/0.5g) sulfamethoxazol dissolved in 5ml of DMSO, placed in a round-bottom flask provided with condenser and refluxed about 8hr, dry it and washed repeatedly with ethanol. Melting point ( $270 - 278^\circ\text{C}$ ), (Guzzo *et al.*, 2021).

Preparation of sec-butyl ((2R,3R,4S,6S)-6-((2-(2-(2,2-dichloroacetamido)-2-hydroxy-1-(4-nitrophenyl) ethoxy)-2-oxoethoxy) methyl)-4-hydroxy-2-methoxy-5-methyltetrahydro-2H-pyran-3-yl) phthalate (S<sub>3</sub>)<sup>18</sup>:

One gm of (S<sub>1</sub>) dissolved in 5ml of DMSO, mixed with ( 0.002 mole 0.4g ) of salbutamol dissolved in DMSO 5ml ,placed in a round-bottom flask provided with condenser and separatory funnel containing about 8hr, then the yellow precipitate washed with ethanol and dried, Melting point ( $199-210^\circ\text{C}$ ). The same procedure is used to prepare different compounds from the reaction of (s) 2-(((2S,4S,5R,6R)-5-((2-(sec-butoxycarbonyl) benzoyl) oxy)-4-hydroxy-6-methoxy-3-methyltetrahydro-2H-pyran-2-yl) methoxy) acetic acid with various drug phenylephrin [S<sub>4</sub>], Trimethoprim [S<sub>5</sub>], Sodium Fusidate [S<sub>6</sub>], Hemayoxiline [S<sub>7</sub>], chloramphenicol [S<sub>8</sub>], (Guzzo *et al.*, 2021).

### Protein Preparation

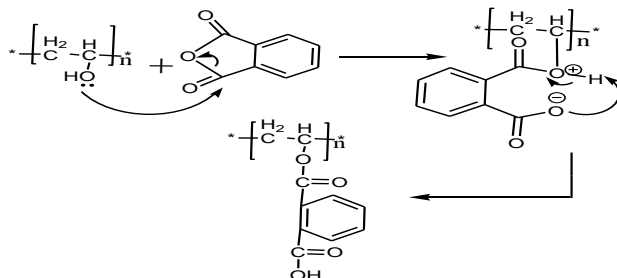
The co-crystal structures of fungi and bacteria have been downloaded from the Protein Data Bank (PDB code: 1IYK and 6TOP, respectively). Proteins were chosen based on the resolution of the published structure and the validation of the crystallized ligand. The "Prepare Protein: protein preparation wizard" Protocol was used to insert any missing loops and atoms, as well as assign 3D coordinates to the structure. All previous results were based on the default parameters of the protocol. The active site was assigned a radius of  $10 \text{ \AA}$  around the bound ligand, which included the active site. Later, the co-crystallized ligand was chosen to identify the active site, and the protein was ready for docking.

### Anti-bacterial Activity Test

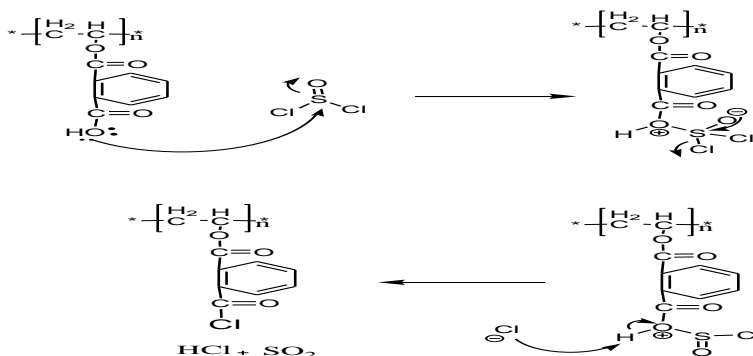
Muller Hinton agar was made by dissolving 38 grams in 1000 ml of distilled water with continuous stirring and heating using a Hot Plate device until complete dissolution was achieved and then placed in an Autoclave device at a temperature of  $121^\circ\text{C}$  and a pressure of 15 atmospheres. The solution was chilled for 15 minutes before being placed onto special "sterile Petri" plates and allowed to harden. The dishes were then contaminated with the prepared isolates and spread evenly across the surface of the medium using a sterile spreader before being allowed to dry. Different concentrations ppm of drug-polymer put in incubated at  $37^\circ\text{C}$  for 24 hours, and the results were recorded by measuring the diameter of inhibition in millimetres with a ruler (Awad *et al.*, 2021).

### 3. RESULTS AND DISCUSSION

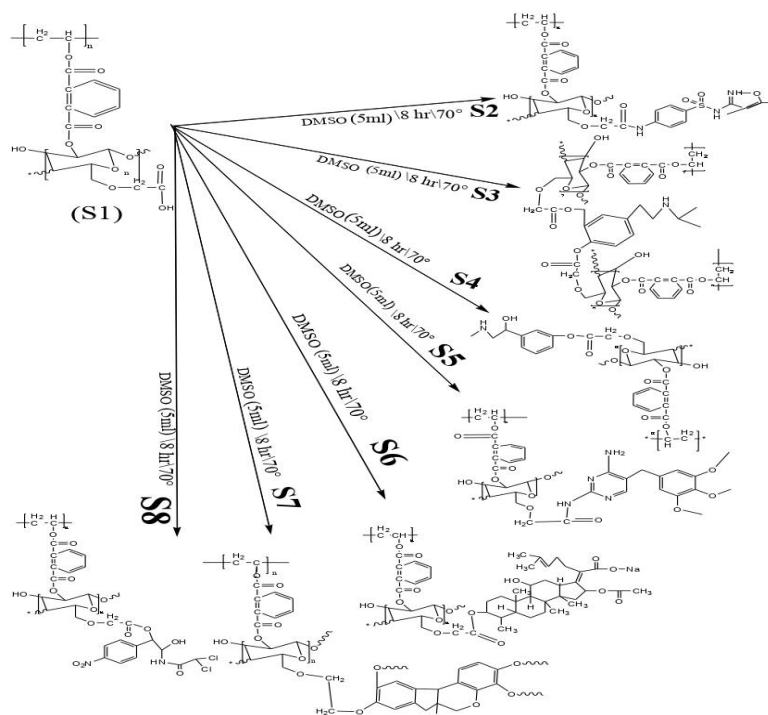
Seven new drug polymers were prepared by modification of PVA with CMC Hydroxyl group in Polyvinylalcohol reacted with carbonyl group in phthalicanhydride by attacking hydroxyl group as nucleophilic to the carbonyl group in phthalicanhydride by ring opening of cyclic anhydride these step illustrated in scheme (1a) , Conversion of carboxylic group to acid chloride using thionyl chloride .This reaction converts a less reactive carboxylic acid in to a more reactive an acid chloride. thionyl chloride converts the OH group of the acid into a better leaving group, it provides the nucleophile ( $\text{Cl}^-$ ) to displace the leaving group. The steps in the process are illustrated in mechanism below scheme 1(b).



Scheme 1(a). Ring opening reaction of cyclic anhydride by hydroxyl group.



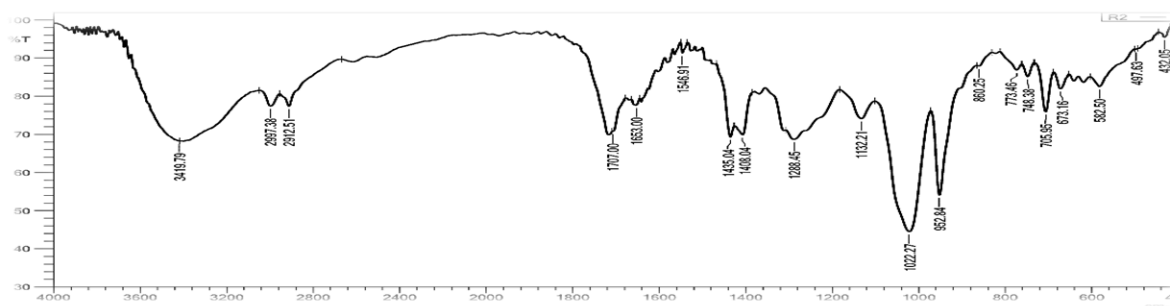
Scheme 1(b). Hydroxyl group in Carboxymethyl cellulose reacted with acid chloride in modification of PVA- to give new modification polymer. Drug polymer preparation by reaction of poly PVA-g-CMC with different drug, these reactions illustrated in scheme 2.



**Scheme 2. Reaction of poly PVA-g- CMC with different hydroxyl drug and different amino drugs.**

#### Fourier Transform Infrared Spectra (FT-IR)

The significant FTIR spectral data comprising the compounds pertinent vibrational bands in the region of 4000-400  $\text{cm}^{-1}$ , in Table 2. (S1) in Figure (1) showed absorption at 3419  $\text{cm}^{-1}$  assigned to the -OH stretching group, 2997-2912  $\text{cm}^{-1}$  were asymmetrical and symmetrical stretching of (C-H) aliphatic, 1707  $\text{cm}^{-1}$  represented to stretching vibration of (C=O) ester. (S2) in Figure (2) showed the absorption band around 3371  $\text{cm}^{-1}$  assigned to the NH-amine, two band attributed to asymmetrical and symmetrical stretching of (C-H) aliphatic at 2983-2914  $\text{cm}^{-1}$ , (C-H) aromatic peak around at 3062  $\text{cm}^{-1}$ , band at 1786  $\text{cm}^{-1}$  represented stretching vibration of (C=O) carbonyl of ester, band at 1712  $\text{cm}^{-1}$  represented stretching vibration of (C=O) carboxylic group, band at 1614  $\text{cm}^{-1}$  attributed to amide group. (S3) in Figure (3) showed absorption at 3375  $\text{cm}^{-1}$  assigned to the -OH stretching group, 2916-2980  $\text{cm}^{-1}$  were asymmetrical and symmetrical stretching of (C-H) aliphatic, 1718  $\text{cm}^{-1}$  represented to stretching vibration of (C=O) ester. (S4) in Figure (4). show absorption at 3429  $\text{cm}^{-1}$  assigned of (OH) group, another peaks appeared at 2960-2806  $\text{cm}^{-1}$  due to the asymmetrical and symmetrical stretching of (C-H) aliphatic, (C-H) aromatic peak around at 3015  $\text{cm}^{-1}$ , the absorption of (C=O) ester was appeared at 1718  $\text{cm}^{-1}$ . (S5) in Figure (5) showed absorption at 3412  $\text{cm}^{-1}$  due to the (NH<sub>2</sub>) amine, 2837-2939  $\text{cm}^{-1}$  were asymmetrical and symmetrical stretching of (C-H) aliphatic, band at 1726  $\text{cm}^{-1}$  represented stretching vibration of (C=O) carbonyl of amide group (Awad *et al.*, 2021; Daoud, 2023).



**Figure 1. FT-IR of Compound (S1).**

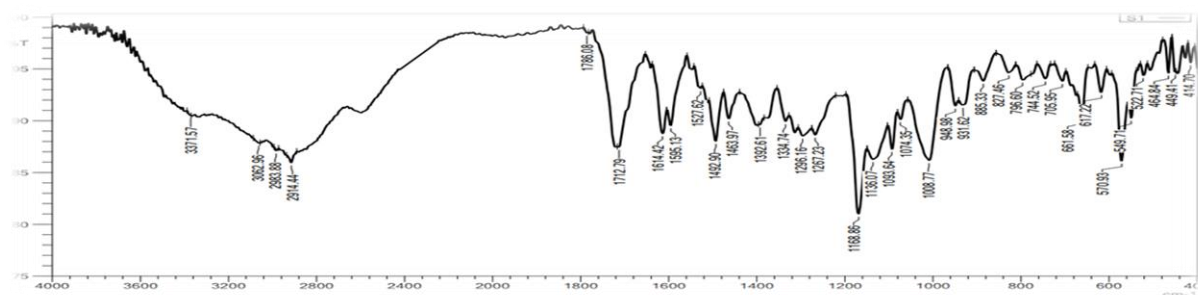


Figure 2. FT-IR of Compound (S2).

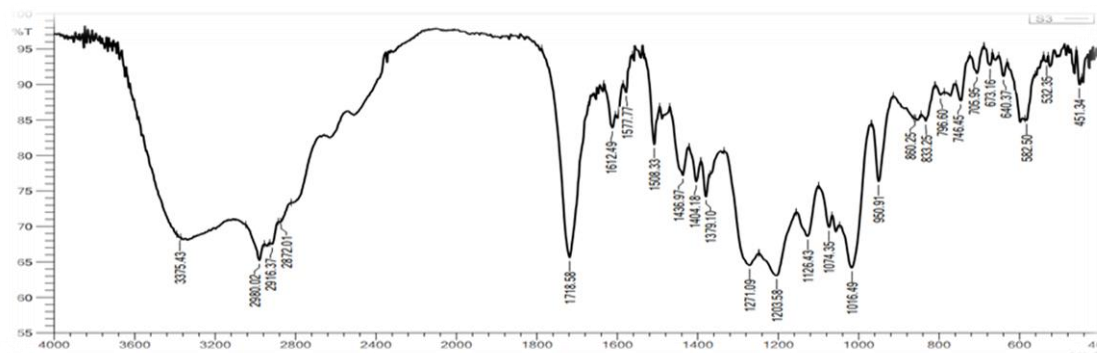


Figure 3. FT-IR of Compound (S3).

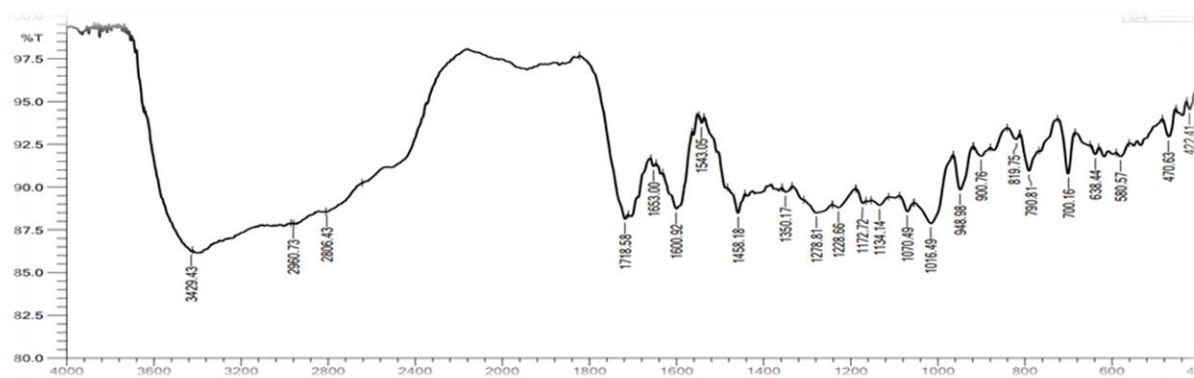


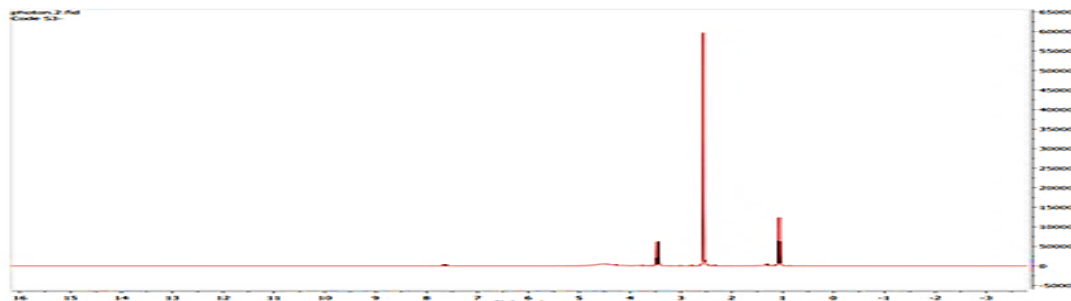
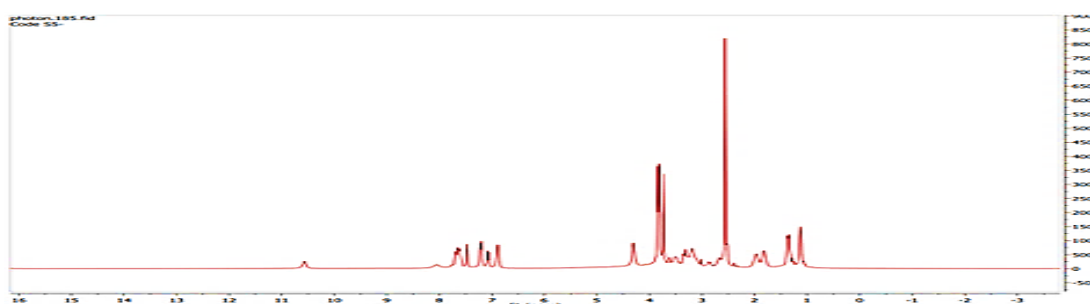
Figure 4. FT-IR of Compound (S4).

Table 2. FT-IR spectral data of synthesized compounds [S1-S8].

NO. .	$\nu$ (O-H) $\text{cm}^{-1}$	N-H) ( $\nu$ $\text{cm}^{-1}$	$\nu$ (C-H) $\text{cm}^{-1}$ aromatic	$\nu$ (C-H) $\text{cm}^{-1}$ aliphatic	$\nu$ (C=O) $\text{cm}^{-1}$ ester	$\nu$ (C=C) $\text{cm}^{-1}$	$\nu$ (C-O) $\text{cm}^{-1}$
S1	3419	_____	3012	2997-2912	1707	1653	1288
S2	_____	3371	3062	2983-2914	1786	1614	1296
S3	3375	_____	3044	2916-2872	1718	1612	1271
S4	3429	_____	3015	2960-2806	1718	1653	1278
S5	_____	3412	3032	2939-2837	1726	1645	1271
S6	3414	_____	3075	2931-2834	1714	1641	1255
S7	3427	_____	3010	2929-2814	1714	1637	1222
S8	3396	_____	3064	2943-2845	1703	1602	1280

**Proton Nuclear Magnetic Resonance ( $^1\text{H-NMR}$ )**

$^1\text{H-NMR}$  spectra of some polymers were obtained using DMSO- $d_6$  as a solvent, they were illustrated as shown: The  $^1\text{H-NMR}$  spectrum of the polymer [S<sub>3</sub>] was shown in Figure (5), which shows the following peaks:  $\delta$  1.2-1.6ppm (CH-CH, 2H, m),  $\delta$  2.5ppm (CH<sub>2</sub>-CH, 3H, t),  $\delta$  3.8ppm (NH-CH, 1H, s),  $\delta$  4.9ppm (R-OH, 1H, s),  $\delta$  7.9-8.2 ppm (CH arom, 1H, s). The  $^1\text{H-NMR}$  spectrum of the prepared polymer [S<sub>5</sub>] was shown in Figure. (6), which shows the following peaks:  $\delta$  1.1-1.5ppm (CH<sub>2</sub>-CH, 3H, m), 2.4ppm (CH-CO, 1H, s),  $\delta$  3.8-4.1ppm (NH-CH, 1H, m),  $\delta$  7.1-7.9 ppm (CH arom, 1H, s),  $\delta$  10.5 ppm (Ar-OH, 1H, m).

Figure 5.  $^1\text{H-NMR}$  of Compound (S<sub>5</sub>).Figure 6.  $^1\text{H-NMR}$  of Compound (S<sub>3</sub>).**Ultra Violet spectra of compound (S<sub>3</sub>, S<sub>5</sub>)**

They are listed in Table 3. The spectra indicated a strong absorption band at 270-320 nm, which was caused by the  $n-\pi^*$  transition, and an absorption band at 210-245 nm. was caused by the  $\pi-\pi^*$  transition <sup>19,20</sup> Figureures 7,8, show the Ultra. Violet spectrum to in pH=9 and pH=4.

**Table 3. UV absorption.**

Code No.	$\lambda$ Max nm	
	$n-\pi^*$	$\pi-\pi^*$
S3 (PH=4)	285	245
S3 (PH=9)	282	245

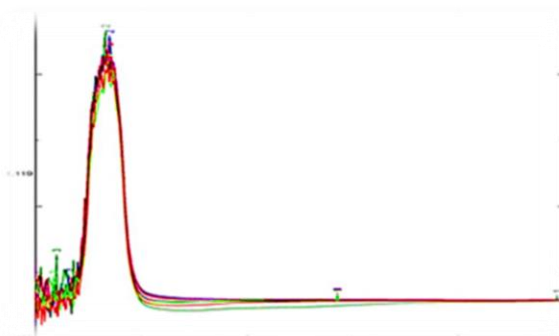


Figure 7. Ultra Violet spectra (S3) in pH=9.



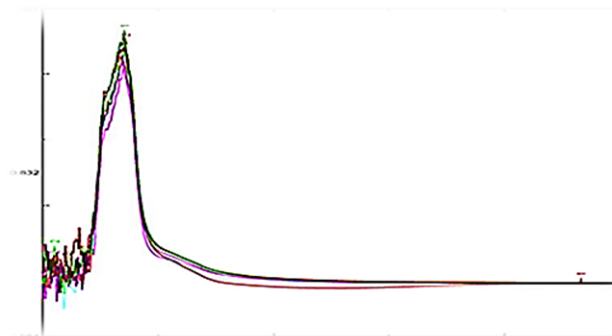


Figure 8. Ultra Violet spectra (S3) in pH=4.

### Controlled Drug Release

The 0.1 gm sample was immersed continuously in 100ml of solution at 30°C-40°C to examine drug delivery for produced drug polymers. In order to track the delivery time, the wave length of max was measured with a UV spectrometer at various times and pH levels. The highest quantity of drugs accessible for release was established by the weight loss as a function of time relationship. The impact of pH values on the rate of release and profiles of weight % present in the sample against time at pH 4 and 9 at 37°C was studied using drug condensed polymer, S<sub>3</sub>, S<sub>5</sub> as shown in Figures 9,10. The amides that were hydrolyzed in the presence of a base cleaved more than acidic amides.

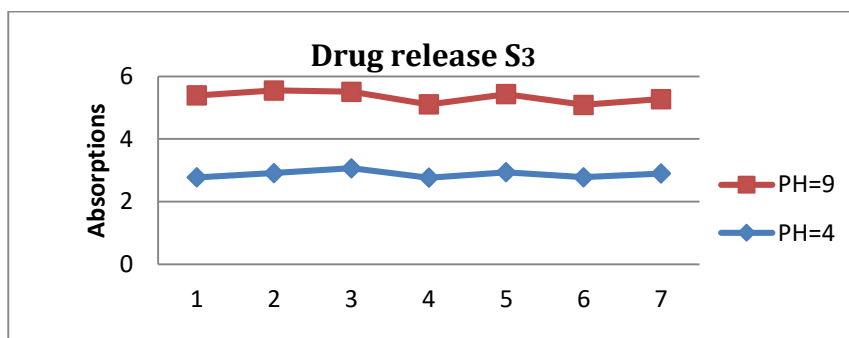


Figure 9. Controlled release of S<sub>3</sub> drug polymers in pH (4&9), 7 days.

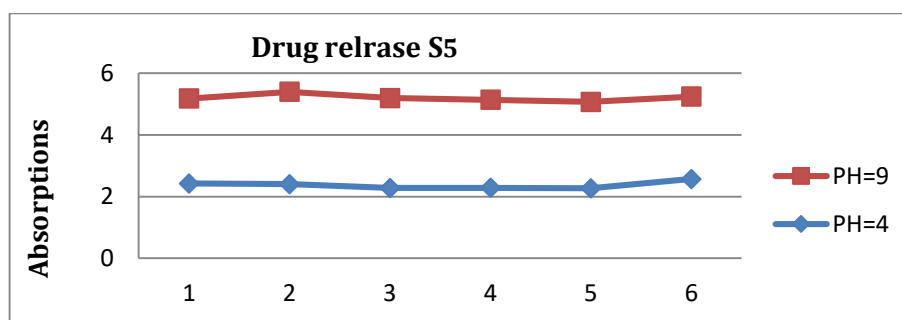


Figure 10. Controlled release of S<sub>5</sub> drug polymers in pH(4&9), 7 days.

### Study of Thermal Properties

Thermogravimetric (TG) curves of polymers [S<sub>3</sub>, S<sub>5</sub>] in table 4 were recorded under argon at temperatures between 0 and 1000 °C. At a heating rate of 10 °C. min<sup>-1</sup>, nearly all of the prepared polymers demonstrated good thermal stability. The weight loss in polymer S<sub>3</sub> was shown in three main stages by the TGA curves (Figure 11): The first step (120-130) has weight losses of around (26.52 %). The ester bond decomposed at 270-275°C, resulting in a weight loss of approximately (51.66%). The final one has weight losses of roughly (9.121%) and a major chain disintegration temperature range of (450–600°C), (Awad *et al.*, 2021).

The TGA curves for polymer S<sub>5</sub> in (Figure 12) demonstrated five main phases of weight loss: the ester bond breakdown (230°C) and weight loss of around (16.66%); The first step (97) has weight losses of around (3.465%). Weight loss of around (4.699%) and temperature changes of (150) °C are associated with the second stage. The ester second bond breakdown

(350°C) and weight loss of approximately (62.56%). The final one has weight losses of roughly (11.40%) and a disintegration of the polymer's main chain between (450-600 °C).

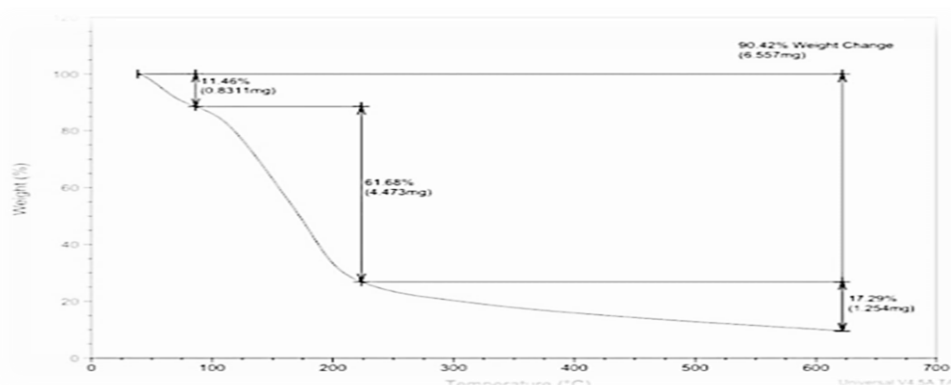


Figure 11. TGA for prepared polymer S3.

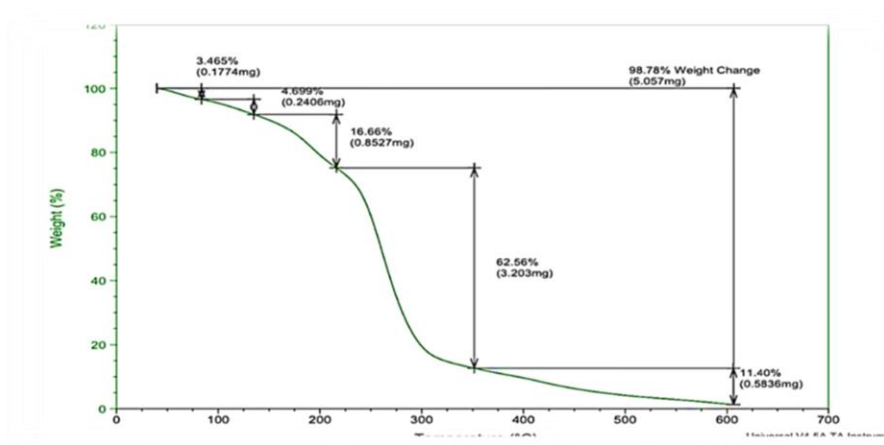


Figure 12 .TGA for prepared polymer S5.

Codes No.	Temp. c°	Weight Loss%
S3	120-130	26.52
	270-275	51.66
	450-600	9.121
S5	97	3.465
	150	4.699
	230	16.66
	350	62.56
	610	11.40

Table 4. Thermogravimetric (TG) curves.

### Compounds Preparation

ChemDraw-20 was utilized for drawing seven compounds, which were followed by imported into (MOE) 2014 and converted into the appropriate 3D structures using the "prepare ligand" process. This method was utilized for a range of tasks, including assigning proper bond ordering, producing ionization states, and assigning chemical isomers, conformations, and tautomers. Except for pH-based ionization, which was adjusted to 7.2-7.6, the default settings were used (Daoud,2023).

### Docking validation



It is the process by which the docking process is verified by comparing the ligand pose from docking (under different algorithm) with ligand from crystal form, through the RMSD (Root Mean Square Deviation) value as shown in table 5. Aim of this method to make docking results more reliable

**Table 5. RMSD calculation.**

Target	RMSD
1IYK	2.72
6top	1.67

### Molecular docking

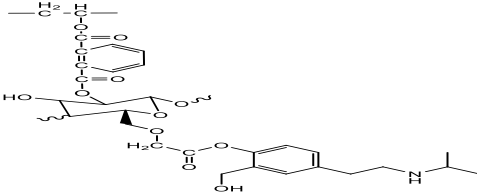
In drug discovery, molecular docking is a computational approach that predicts interactions between a target protein and small molecules. The latter constitute ligands and the former are receptors. This aims to determine the strength with which the receptor binds to its corresponding ligand as well as identify the preferred Compound between them. The Rigid receptor algorithm is a strong docking algorithm found in the (MOE) 2014. It is based on physics which makes it possible for ligand-receptor interactions to be evaluated. These include hydrogen bonding, van der Waals forces and electrostatic interactions, among other things that are considered by Rigid receptor algorithm. The best binding pose can be identified through sampling different ligand conformations and orientations. After the compounds is prepared and grid generate is employed the docking process is beginning. Dock the synthesized compounds into the active sites for fungi target (PDB code: 1IYK) and for bacteria target PDB code: 6TOP). After that we could analyze whether they are able to bind, and at what rate. To find out the possible lead for future, (Awad *et al.*, 2021). work.

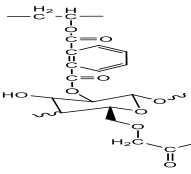
Codes..... No.....	Temp. °C.....	Weight..... Loss %
S3	120-130	26.52
	270-275	51.66
	450-600	9.121
S5	97	3.465
	150	4.699
	230	16.66
	350	62.56
	610	11.40

### Compounds Preparation

Seven compounds were proposed as antibacterial and antifungal candidates as shown in Table 6. Thereafter, 2D drawings were created using Chem Draw software, which were subsequently converted to 3D structures using (MOE) 2014. Following that, the recommended compounds were generated using the "ligprepare" protocol, with all settings set to default, allowing the process to modify ionization similar to a biological system and generating conformations, isomers, and tautomers. The final number of ligands ready for docking into the active site of targeted proteins in bacteria and fungus was twelve, including the co-crystal structures with 6TOP and 1IYK (Bufaroosha *et al.*, 2020).

**Table 6. List of synthesized compounds.**

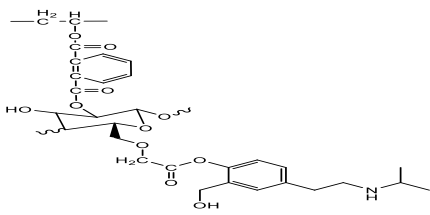
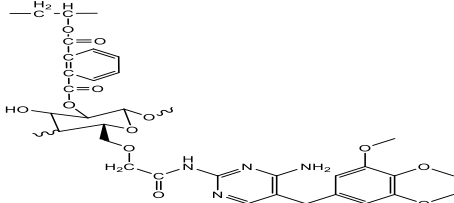
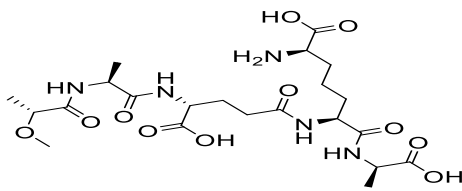
#No	2D structure	Code_name	Drug moiety
1		S3	Salbutamol

2		S5	Trimethoprim
---	---	----	--------------

### Molecular Docking

All the suggested compounds including co-crystal ligands were docked using "Rigid receptor" algorithm and compounds were synthesized and tested against bacteria and fungi growth. Molecular docking in (MOE) 2014, particularly with "Rigid receptor" Docking, entails predicting the preferred orientation of one molecule to another when bonded together to form a stable compound. It is a technique often used in drug discovery to anticipate the binding mechanism and affinity of small compounds for a target protein. "Rigid receptor" Docking in (MOE) 2014 is well-known for its remarkable accuracy and dependability in predicting binding energies and interactions between ligands and proteins.

**Table 7. Computational result of the targeted compounds against bacteria with native ligand (as reference for the computational run).**

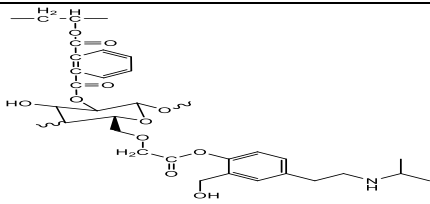
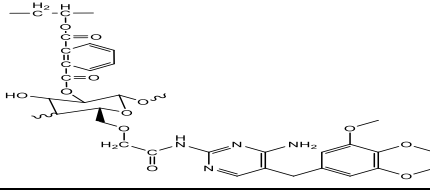
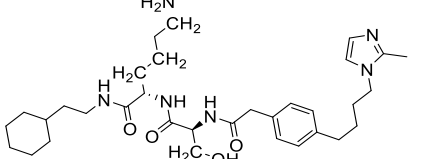
Name	2D structure	Dock score interaction energy
#5 S3		-5.468
#7 S5		-5.729
#8 native_ligand_6Top		-6.927

As displayed in Table 7, compound S5 is the second highest docking score of the synthesized compound. By using view interactions tool within (MOE) 2014, many interactions were performed by compound S5. These interactions with the active site were H-bond interaction between oxygen and Pro 580 while nitrogen of pyrimidine ring with LYS 616, and Pi-H interaction between Benzene ring and Tyr 583.

As shown in Table 7, compound S3 had a docking score -5.468 of the designed compound but less than the reference ligand 6TOP. By using view interactions tool within (MOE) 2014, two interactions were performed by compound S3. These interactions with the active site were H- bond interaction between carbonyl of terminal ester and Asp 581 and hydroxyl of oxazole ring with Lys 616.

**Table 8. computational result of the targeted compounds against fungi with native ligand (as reference for the computational run).**

Name	2D structure	Dock score interaction energy
------	--------------	-------------------------------

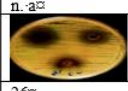
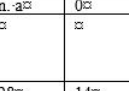
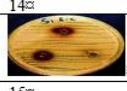
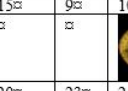







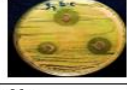

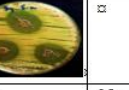






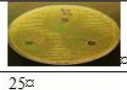






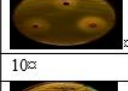

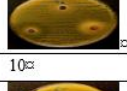
















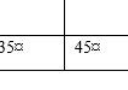

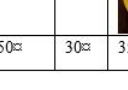

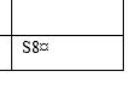












#5 S3		-9.038
#7 S5		-8.858
#8 native_ligan d_1IYK		-7.949

As presented in Table 8, compound S3 had docking score -9.038 of the designed compound but highest than the reference ligand 1IYK. By using view interactions tool within (MOE) 2014, two H- bond interactions were performed by compound S3. These interactions with the active site were H-bond between carbonyl of ester with Gly 413 and nitrogen of terminal secondary amine with His 242. As presented in Table 8, compound S5 had docking score -8.858 of the designed compound highest than the reference ligand 1IYK. By using view interactions tool within (MOE) 2014, interaction was performed by compound S5. The only interaction with the active site were H-bond interaction between nitrogen of amide with Asp 412.

### The Biological Activity

The newly developed compounds showed great promise against fungus and bacteria. These substances are essential components of various bioactive molecules utilized in medicine and material science. Compounds(S4,S5,S8) shown excellent action against E. Coli, while compounds (S3,S7,S8) displayed excellent activity against Antifungal candida and compounds S3 ,S4,S5,S6 and S7,S8 showed noteworthy efficacy against Candida albicans . Different amounts of Staphylococcus aureus were present in every synthetic substance (Awad *et al.*, 2021).

Table 7. The effectiveness of antibacterial.

C. albicans (fungus)			E. coli (-ve)			S. aureus (+ve)			Compounds
→ 25%	50%	100%	25%	50%	100%	25%	50%	100%	
n.a	n.a	n.a	0	14	15	9	10	10	S2
									
23	26	28	14	15	20	23	24	25	S3
									
n.a	n.a	n.a	30	30	35	25	30	35	S4
									
0	0	10	17	25	27	20	25	28	S5
									
10	10	10	10	10	15	30	30	27	S6
									
0	15	16	15	16	17	23	30	30	S7
									
27	30	35	45	45	50	30	35	40	S8
									

\*n. a = no. activity

#### 4. CONCLUSION

Based on our docking data, S4 shows remarkable antifungal activity with a docking score of -10.172 and antibacterial capabilities in compound with Phenylephrine, with a docking score of -4.997. Conversely, S2 compound with Sulfamethoxazole has the best antibacterial activity between synthesized complexes when as evidenced by its docking score of -6.750. Furthermore, S2 with Sulfamethoxazole has significant antifungal with docking score -9.027. which indicates that S2 compound with Sulfamethoxazole has broad-spectrum antimicrobial activity due to its antibacterial and antifungal characteristics. As a result, our complex appears to possess greater potential for antifungal applications compared to antibacterial ones.

**Acknowledgments :** The authors thank the chairman and colleagues of the Department of Chemistry, College of Science for Women , University of Baghdad for their assistance and support.

**Funding:** Thier is no funding.

#### Authorship contribution

Rasha Sh. Nayyef contributed to the idea, data curation, investigation, methodology, software development, and project supervision. Sana H. Awad specializes in document validation, writing, review, and editing. Rasha Sh. Nayyef &Sana H. Awad contributed to the project by providing visualization, writing the original text, and reviewing and correcting the content.

**Conflict of Interest:** The authors assert that they have no conflict of interest.

#### REFERENCES

- [1] Kumar B, Negi YS (2018) Water absorption and viscosity behaviour of thermally stable novel graft copolymer of carboxymethyl cellulose and poly(sodium 1-hydroxy acrylate). Carbohydr. Polym. 181: 862–870. <https://doi.org/10.1016/j.carbpol.2017.11.066>
- [2] Saha N, Shah R, Gupta P, Mandal BB, Alexandrova R, Sikiric MD, Saha P(2019) PVP-CMC hydrogel: An excellent bioinspired and biocompatible scaffold for osseointegration. Mater. Sci. Eng. 95: 440–449. <https://doi.org/10.1016/j.msec.2018.04.050>
- [3] Rahman MS, Hasan MS, Nitai AS, Nam S, Karmakar AK, Ahsan MS, Shiddiky MJA, Ahmed MB (2021) Recent Developments of Carboxymethyl Cellulose. Polymers. 13(8):1345. <https://doi.org/10.3390/polym13081345>
- [4] Elena-Emilia T, Cristina-Elena DN, Mădălina Georgiana AK, Lăcrămioara P, Valentina A, Mihai PR, Violeta GM (2021). An Overview of Cellulose Derivatives-Based Dressings for Wound-Healing Management. Pharmaceuticals. <https://doi.org/10.3390/ph14121215>
- [5] Jiamin W, Zhaoxue F, Chaohong D, Ping Z, Jianhui Q, Longxiang Z (2022) Synthesis of Sodium Carboxymethyl Cellulose/Poly(acrylic acid) Microgels via Visible-Light-Triggered Polymerization as a Self-Sedimentary Cationic Basic Dye Adsorbent. Langmuir. 38 (12):3711-3719. <http://doi.org/10.1021/acs.Langmuir.1c03196>
- [6] Sirajudheen P, Karthikeyan P, Vigneshwaran S, Meenakshi S(2020) Synthesis and characterization of La (III) supported carboxymethylcellulose-clay composite for toxic dyes removal: Evaluation of adsorption kinetics, isotherms and thermodynamics. Int. J. Biol. Macromol. 161:1117–1126. <https://doi.org/10.1016/j.ijbiomac.2020.06.103>
- [7] Sirajudheen P, Nikitha MR, Karthikeyan P, Meenakshi S (2020) Perceptive removal of toxic azo dyes from water using magnetic Fe<sub>3</sub>O<sub>4</sub> reinforced graphene oxide–carboxymethyl cellulose recyclable composite: Adsorption investigation of parametric studies and their mechanisms. Surf. Interfaces. 21:100648. <http://doi.org/10.1016/j.surf.2020.100648>
- [8] Kong Q, Preis S, Li L, Luo P, Hu Y, Wei C (2020) Graphene oxide-terminated hyperbranched amino polymer-carboxymethyl cellulose ternary nanocomposite for efficient removal of heavy metals from aqueous solutions. Int. J. Biol. Macromol. 149: 581–592. [DOI:10.1016/j.surf.2020.100648](mailto:DOI:10.1016/j.surf.2020.100648)
- [9] Zong P, Cao D, Cheng Y, Wang S, Zhang J, Guo Z, Hayat T, Alharbi NS, He C (2019) Carboxymethyl cellulose supported magnetic graphene oxide composites by plasma induced technique and their highly efficient removal of uranium ions. Cellulose. 26: 4039–4060. <http://doi.org/10.1007/s10570-019-02358-4>
- [10] Tanzifi M, Yarak MT, Beiramzadeh Z, Saremi LH, Najafifard M, Moradi H, Mansouri M, Karami M, Bazgir H (2020) Carboxymethyl cellulose improved adsorption capacity of polypyrrole/CMC composite nanoparticles

- for removal of reactive dyes: Experimental optimization and DFT calculation. *Chemosphere*. 255: 127052. <mailto:https://doi.org/10.1016/j.chemosphere.2020.127052>
- [11] Godiya CB, Cheng X, Li D, Chen Z, Lu X (2019) Carboxymethyl cellulose/polyacrylamide composite hydrogel for cascaded treatment/reuse of heavy metal ions in wastewater. *J. Hazard. Mater.* 364:28–38. <http://doi.org/10.1016/j.jhazmat.2018.09.076>
- [12] Janarthanan G, Tran HN, Cha E, Lee C, Das D, Noh I (2020) 3D printable and injectable lactoferrin-loaded carboxymethyl cellulose-glycol chitosan hydrogels for tissue engineering applications. *Mater. Sci. Eng. C*. 113:111008. <http://doi.org/10.1016/j.msec.2020.111008>
- [13] Awad SH, Hussein FA, Mustafa SA (2021) Synthesis, Characterization of Poly (chitosan nano-particles-co-pyruvic acid) and Substitution with Different Amino Acids .*International Journal of Drug Delivery Technology*. 11(4):1313–1317 . <http://doi.org/10.25258/ijddt.11.4.32>
- [14] Al-Sahib SA, Awad SH (2022) Synthesis, Characterization of Chitosan para- hydroxyl Benzaldehyde Schiff Base Linked Maleic Anhydride and the Evaluation of Its Antimicrobial Activities. *Baghdad Science Journal*. 19(6):1265–1275. <https://doi.org/10.21123/bsj.2022.5655>
- [15] Liu B, Xu H, Zhao H, Wei L, Zhao L, Li Y (2016) Preparation and characterization of smart starch/PVA films for simultaneous colorimetric indication and antimicrobial activity for food packaging applications. *Carbohydrate Polyme.* <https://doi.org/10.1016/j.carbpol.2016.10.067>
- [16] Guzzo M, Simon N, Ye L, Motcho J, Bokanski B (2021) Improved release of poorly water-soluble drug by using electrospun water-soluble polymers as carriers *Pharmacy*. 14(1):34. <https://doi.org/10.3390/pharmaceutics14010034>
- [17] Awad Sh, Hamood F, Kareem SASA. (2021) Synthesis and Characterization of Co-polymer of (Albumin-PVP) as Carriers for Different Antibiotics. *Int J Drug Deliv Technol.* 11(4): 137982 .<http://doi.org/10.25258/ijddt.11.4.43>
- [18] Daoud RD (2023) Determining the Ionization Constants of Some Schiff Bases Derived from Vanillin and Aniline and Its Substitutes by Spectrometric Titration Method.(Hammett Relation Application).*Coll Basic Educ Res J*. 19 (1): 844-60. <http://doi.org/10.33899/berj.2023.178143>
- [19] Bufaroosha M, Salih N, Hadi AG, Ahmed SD, Al-mashhadani MH, Yousif E (2020) The Effect of UV Aging on the Structure of PVC in the Presence of Organotin (IV) Compounds. *AL-Nahrain J. Sci.* 23(1):5761. <http://doi.org/10.22401/ANJS.23.1.08>